Dependence of the Core Radial Electric Field on Ion and Electron Temperature in W7-X

N.A. Pablant[1], A. Langenberg[2], A. Alonso[5], J. Baldzuhn[2], C.D. Beidler[2], M. Bitter[1], S. Bozhenkov[2], K.J. Brunner[2], R. Burhenn[2], A. Dinklage[2], G. Fuchert[2], D.A. Gates[1], J. Geiger[2], K.W. Hill[1], M. Hirsch[2], U. Hoefel[2], Y. Kazakov[8], J. Knauer[2], H. Laqua[2], M. Landreman[4], S. Lazerson[1], H. Maassberg[2], O. Marchuk[6], E. Pasch[2], A. Pavone[2], S. Satake[3], T. Schroeder[2], J. Svensson[2], P. Traverso[7], Y. Turkin[2], J.L. Velasco[5], A. Von Stechow[2], F. Warmer[2], G. Weir[2], R.C. Wolf[1], D. Zhang[2] and the W7-X Team

[1]*Princeton Plasma Physics Laboratory, Princeton, NJ, USA*
[2]*Max-Planck-Institut für Plasmaphysik,Greifswald, Germany*
[3]*National Institute for Fusion Science, Toki, Japan*
[4]*University of Maryland, College Park, MD, USA*
[5]*Laboratorio Nacional de Fusión – CIEMAT, Madrid, Spain*
[6]*Forschungszentrum Jülich , Jülich, Germany*
[7]*Auburn University, Auburn, AL, USA*
[8]*Chalmers University of Technology, Göteborg, Sweden*

I. Introduction

The core radial electric field (E_r) plays an important role in stellarator plasmas, and is expected to have a strong effect on heat, particle and impurity fluxes[1]. Because the neoclassical particle fluxes in a stellarator are not intrinsically ambipolar, the E_r is strongly tied to the ion and electron temperature and density profiles[2]. In W7-X, a large positive radial electric field is expected in cases in where $T_e \gg T_i$, while a negative electric field is expected when the temperatures are close to equal, $T_e \approx T_i$[3]. This dependence of E_r on the temperatures is investigated experimentally in W7-X by looking at a single plasma program with hydrogen pellet fueling in which a wide range of plasma temperatures and densities were achieved. These results represent the first measurements of E_r in W7-X plasmas with an installed island divertor.

II. Diagnostic Method

Determination of the E_r profile is made possible by utilizing the X-Ray Imaging Crystal Spectrometer (XICS)[4, 5]. This diagnostic is able to measure perpendicular plasma flow ($u_\perp$), which is closely related to the radial electric field through the radial force balance (see Eq.1).

The XICS diagnostic relies on spectral emission from highly charged argon ions introduced into the plasma. Line integrated flow velocity profiles are found from the Doppler shift of the spectral lines. Through tomographic inversion, using a known plasma equilibrium, it is possible to infer the local plasma flow from these line integrated data. The procedures used for spectral analyses and tomographic inversion, including the inclusion of asymmetries of the perpendic-

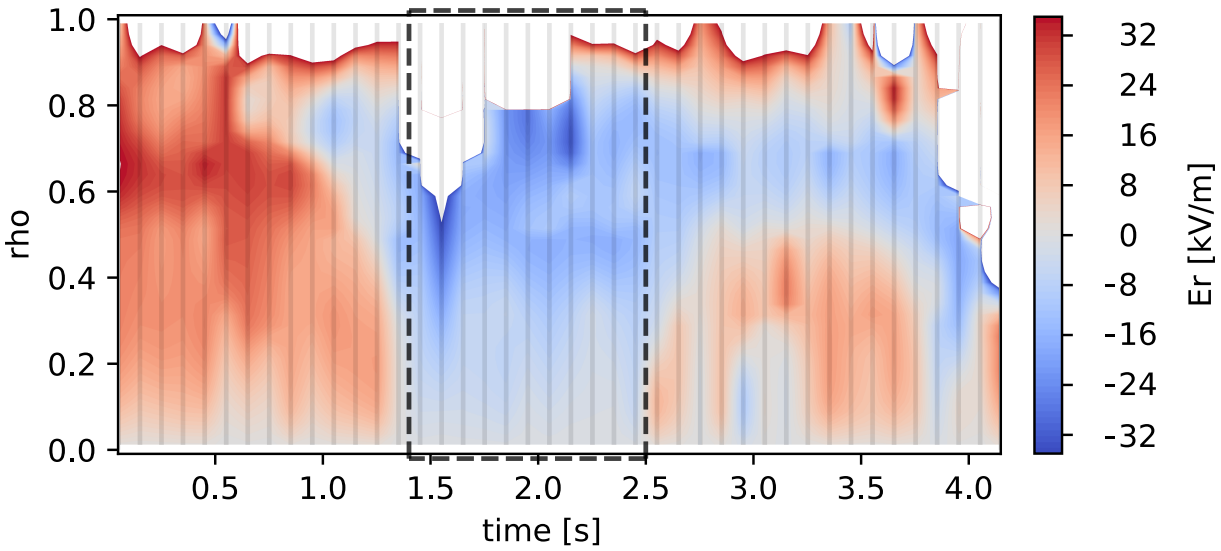

Figure 1: *Inverted radial electric field as inferred from XICS measurements. Raw data has been binned prior to inversion to provide* 100 ms *time resolution and* 3 cm *spatial resolution. Vertical lines denote actual measurement times (center of integration window); color between lines is interpolated. In the time around after* 1.5 s *a strong peaking in the* Ar^{16+} *emissivity profile results in a limited measurable profile extent; radii with insufficient signal for valid measurements are left white. The dashed box indicates the time window in which the plasma is fully within the ion-root regime.*

ular velocity on a flux surface[6], are described in detail in Refs. 4, 5, 7, 8. For the particular geometry of the XICS sightlines on W7-X, inversions are not sensitive to finite pressure effects on the equilibrium; therefore a vacuum VMEC equilibrium is used for all inversions shown in the current work.

To derive the radial electric field from the flux surface averaged perpendicular flow velocity the radial force balance equation can be used.

$$\langle E_r \rangle = \frac{1}{e n_I Z_I} \frac{\partial p_I}{\partial \rho} \langle |\nabla \rho| \rangle - \langle u_\perp B \rangle \tag{1}$$

Where p_I, n_I and Z_I denote the pressure, density and charge of the ion species being measured. The pressure gradient term is small for measurements of argon with the flat pressure profiles seen at W7-X, and has been neglected in the results shown in this work. The XICS viewing geometry, as seen in Ref. 5, Fig.1, is primarily sensitive to the component of the velocity that is perpendicular to the magnetic field lines. Given this insensitivity, the parallel velocity is ignored except for a constant correction which is combined with a more general wavelength calibration correction.

III. Radial Electric Field Measurements

In order to investigate the radial electric field under the widest available range of plasma profiles, a plasma program including cryogentic hydrogen pellet injection[9] and central ECRH heating is chosen for this inital analysis: 20171207.006. This program is of particular interest in

studying the evolution of the radial electric field as it encompasses a wide range of both plasma densities and electron-ion temperature ratios. Due to hardware restrictions on the pellet injection system available during the Op1.2a experimental campaign, the pellet fueling phase of this program is limited to a length of approximately half a second. This limitation results in a highly transient high density phase in the plasma evolution. Even though the plasma conditions are non-stationary, the neoclassical radial electic field is expected to change on the same timescale as the temperature and density evolution.

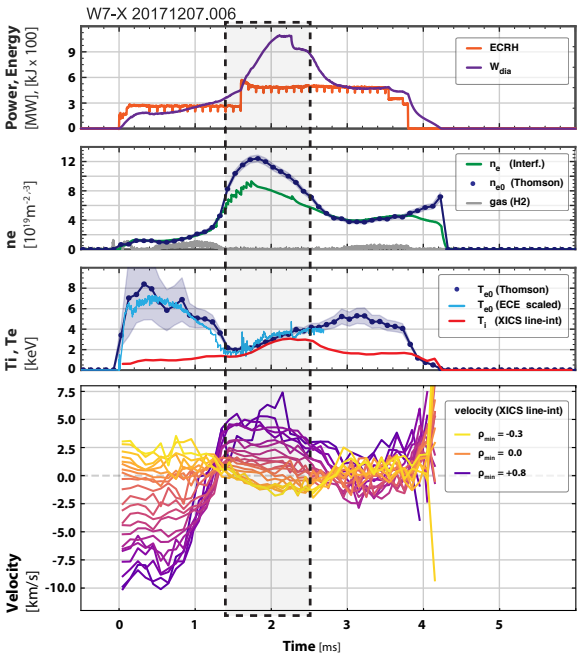

Figure 2: *Time traces for a centrally heated W7-X discharge with hydrogen pellet fueling. Electron temperature and density taken from the central Thomson channels. The absolute value of the ECE temperatures are un-calibrated, and have been scaled to match Thomson measurement. The line-integrated velocities, as measured by XICS, are shown for individual sightlines; Purple and yellow lines represent views above and below the magnetic axis respectively. The dashed box highlights the time in which ion-root conditions are observed.*

Radial electric field profiles inferred from the XICS diagnostic confirm the expected existence of a negative radial electric field in the plasma core (ion-root conditions) during the high-density pellet fueled phase of the program. Measurements of the E_r profile evolution are shown in Fig.1 and Fig.3, and correspond to the plasma program shown in Fig.2. During beginning and ending phases of this program, where the plasma density is lower and $T_e \gg T_i$, a positive core radial electric field is observed. However, in the high density phase of the program temperature equilibration is achieved and an negative radial electric field is developed.

The ion-root phase of this program, in which the radial electric field is negative all the way into the plasma core, exists between 1.40 s and 2.50 s, as seen in Fig.1. The precise timing of the ion-root phase has been determined using an analysis completed using a 20ms integration time (not shown in the current paper), and is expected to be accurate to within this resolution. At the point in which the full ion-root condition develops, at 1.40s, the following plasmas parameters are observed: $T_{eo} = 2.25\,\mathrm{keV}$, $T_{io} = 1.75\,\mathrm{keV}$, $\bar{n}_e \approx 0.6 \times 10^{20}\,\mathrm{m}^{-3}$ and $P_{ECRH} = 2.7\,\mathrm{MW}$. At the start of the transition out of the ion root, at 2.50 s, the following plasma parameters are observed: $T_{eo} = 4.25\,\mathrm{keV}$, $T_{io} = 3.75\,\mathrm{keV}$, $\bar{n}_e \approx 0.6 \times 10^{20}\,\mathrm{m}^{-3}$ and $P_{ECRH} = 5.0\,\mathrm{MW}$. Measurements of the central electron temperature and density are taken from the Thomson scattering diagnostic[10]; line inte-

grated measurements of the electron density from the interferometer[11] give similar values at these times.

At both ends of the ion-root phase we find a similar value of the electron density as well as a similar difference between the absolute ion and electron temperatures of approx 0.5 keV. Interestingly, the ratio of input power to electron density, which has been previously suggested as a metric for the transition between ion-root and electron root [12, 13], is quite different between the start and end of the ion-root phase.

Leading up to full development of the ion-root plasma at 1.40 s, it can be observed that an ion root region develops in the outer portion of the plasmas and expands inward. This change in E_r occurs over a time period of around 0.5 s, and can be seen to generally follow the evolution of the central temperature and density values. Similar behavior is seen as the plasma transitions out of the ion-root after 2.50 s and develops an expanding region of positive radial electric field in the core. The detailed time dependence of changes to E_r profile can be more clearly observed by looking directly at the line-integrated plasma flow measurements. Within the resolution of the available measurements, the electron temperature and velocity appear to change simultaneously, which is consistent with the neoclassical understanding of E_r. These observations of changes in the radial electric field profile in response to changing plasma conditions are in line with studies of the radial electric field at different input powers seen on W7-X[5] and LHD[7].

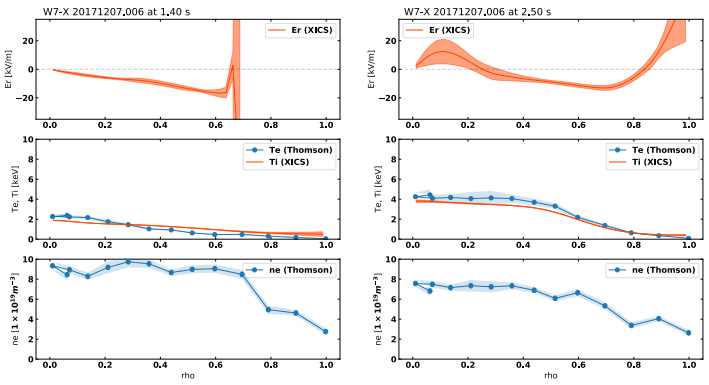

Figure 3: *Plasma profiles near the start and end of the ion-root phase. Radial electric field profiles (E_r) inferred from XICS velocity measurements. Mapping from real space to ρ has been done using a vacuum equilibrium (finite pressure effects ignored).*

Research supported by the U.S. DOE under Contract No. DE-AC02-09CH11466 with Princeton University. This work has been carried out within the framework of the EUROfusion Consortium and has received funding from the Euratom research and training programme 2014-2018 under grant agreement No 633053. The views and opinions expressed herein do not necessarily reflect those of the European Commission.

References

[1] Maaßberg, H. et al. Physics of Plasmas, **16**, 7, 072504 (2009).
[2] Yokoyama, M. et al. Nuclear Fusion, **47**, 9, 1213 (2007).
[3] Turkin, Y. et al. Physics of Plasmas, **18**, 2, 022505 (2011).
[4] Langenberg, A. et al. Review of Scientific Instruments (2018). Accepted for publication.
[5] Pablant, N.A. et al. Physics of Plasmas, **25**, 2, 022508 (2018).
[6] Arévalo, J. et al. Nuclear Fusion, **53**, 2, 023003 (2013).
[7] Pablant, N.A. et al. Plasma Physics and Controlled Fusion, **58**, 4, 045004 (2016).
[8] Pablant, N.A. et al. Review of Scientific Instruments, **85**, 11, 11E424 (2014).
[9] Pedersen, T.S. and et al. Plasma Physics and Controlled Fusion. Submitted for publication.
[10] Pasch, E. et al. 43rd EPS Conference on Plasma Physics, P4.016 (2016).
[11] Krychowiak, M. et al. Review of Scientific Instruments, **87**, 11, 11D304 (2016).
[12] Takeiri, Y. et al. Physics of Plasmas, **10**, 5, 1788 (2003).
[13] Shimozuma, T. et al. Nuclear Fusion, **45**, 11, 1396 (2005).